

Supporting Information

Consecutive oxidative additions of iodine on undulating 2D coordination polymers:
Formation of I-Pt-I chains and inhomogeneous layers

*Ryo Ohtani**, *Riho Yamamoto*, *Hiroyoshi Ohtsu*, *Masaki Kawano*, *Jenny Pirillo*, *Yuh Hijikata*, *Masaaki Sadakiyo*, *Leonard F. Lindoy* and *Shinya Hayami**

Corresponding authors:

R. Ohtani, ohtani@kumamoto-u.ac.jp

S. Hayami, hayami@kumamoto-u.ac.jp

Experimental section

Synthesis

[Mn(salen)]₂[Pt(CN)₄(0.18I₂)] (1) : [Mn(salen)]Cl (141.7 mg, 0.400 mmol) in H₂O (100 mL) was added to K₂[Pt(CN)₄]·3H₂O (75.0 mg, 0.200 mmol) and I₂ (16.0 mg, 0.060 mmol) in MeOH (100 mL) at room temperature. The mixture was stirred for 24h and the dark-brown precipitation that had formed was collected by suction filtration, washed with water then methanol, and dried under vacuum at 550 K to remove lattice water. Yield 32.1%. Anal. Found (calcd) for C₃₆H₃₆I_{0.36}Mn₂N₈O₈Pt (1041.31): C 41.75 (41.48); H 3.25 (3.26); N 10.76 (10.76)%.

[Mn(salen)]₂[Pt(CN)₄(0.45I₂)] (2) : [Mn(salen)]Cl (141.7 mg, 0.400 mmol) in H₂O (100 mL) was added to K₂[Pt(CN)₄]·3H₂O (75.0 mg, 0.200 mmol) and I₂ (25.2 mg, 0.100 mmol) in MeOH (100 mL) at room temperature. The mixture was stirred for 24h, the brown precipitation that had formed was collected by suction filtration, washed with water then methanol, and dried under vacuum at 550 K to remove lattice water. Yield 35.4%. Anal. Found (calcd) for C₃₆H₃₆I_{0.9}Mn₂N₈O₈Pt (1109.84): C 36.92 (36.86); H 2.97 (2.84); N 9.42 (9.56)%.

[Mn(salen)]₂[Pt(CN)₄(0.85I₂)] (3) : [Mn(salen)]Cl (356.7 mg, 1.000 mmol) in H₂O (100 mL) added to K₂[Pt(CN)₄]·3H₂O (188.0 mg, 0.500 mmol) and I₂ (95.0 mg, 0.400 mmol) in MeOH (100 mL) at room temperature. The mixture was stirred for 24h, the dark-green precipitation that had formed was collected by suction filtration, washed with water then methanol, and dried under vacuum at 550 K to remove lattice water. Yield 33.2%. Anal. Found (calcd) for C₃₆H₃₆I_{1.7}Mn₂N₈O₈Pt (1211.36): C 35.85 (35.66); H 2.90 (2.80); N 9.00 (9.02)%.

Physical measurements

Thermogravimetric analysis was performed at 10 K min⁻¹ using a Rigaku Instrument Thermo plus TG 8120 in a nitrogen atmosphere. Elemental analyses (C,H,N) were carried out on a J-SCIENCE LAB JM10 analyzer at the Instrumental Analysis Centre of Kumamoto University. Solid state reflection spectra were recorded with a SCINCO S-2100 spectrophotometer (Shimazu) at room temperature. The microscopic Raman spectroscopy was carried out by LabRAM HR-800 spectrometer (HORIBA Jobin Yvon

Ltd.) at temperatures in the range 100–400 K using an LK-600 hot stage (Linkam). A 785-nm semiconductor laser was used as the excitation source. The diffuse reflectance IR Fourier transform (DRIFT) spectra were recorded in the range of 4000–400 cm^{-1} on a Nicolet ID5 ATR spectrometer. X-ray photoelectron spectroscopy (XPS) was performed using a ULVAC-PHI PHI 5000 Versa Probe-II with a Al- $K\alpha$ X-ray source. The XPS spectra were calibrated using a C1s peak at 284.6 eV. Based on published literatures, XPS peaks were attributed to, M^{2+} or M^{4+} ($M = \text{Pt}$ or Mn) components. We propose that the peaks for Pt^{II} are attributable to divalent ions coordinated to ligands located on the surface of the 2D CPs crystals. Variable temperature powder X-ray diffraction patterns were obtained using the SAGA-LS. The powder samples with homogeneous granularity were sealed in a glass capillary of 0.5 mm internal diameter. Synchrotron radiation (SR) powder diffraction patterns were recorded on an imaging plate (IP) of the large Debye-Scherrer camera installed at BL15 in SAGA-LS. The size of the IP is $200 \times 400 \text{ mm}^2$, which covers up to 72 deg. in 2θ . The pixel size of the IP is $50 \times 50 \mu\text{m}^2$. The radius of the camera is 286.5 mm, which corresponds to 0.01 deg. in 2θ . The energy of the SR was 12.4 keV (wavelength $\lambda = 1.000 \text{ \AA}$). The sample temperatures were controlled by a dry dinitrogen flow using a Rigaku GN_2 apparatus.

Rietveld analysis of **1–3**

The RXPd patterns of **1–3** were indexed using the program DICVOL (A. Boulton, D. Louër, *J. Appl. Crystallogr.* **1991**, *24*, 987-993) to give an orthorhombic unit cell ($a = 14.66700 \text{ \AA}$, $b = 14.66400 \text{ \AA}$, $c = 17.08500 \text{ \AA}$, $V = 3674.588 \text{ \AA}^3$) for **1**, an orthorhombic unit cell ($a = 14.69901 \text{ \AA}$, $b = 14.44100 \text{ \AA}$, $c = 17.54748 \text{ \AA}$, $V = 3724.773 \text{ \AA}^3$) for **2**, and an tetragonal unit cell ($a = b = 14.55186 \text{ \AA}$, $c = 17.65986 \text{ \AA}$, $V = 3739.595 \text{ \AA}^3$) for **3**, with good figure of merit. The space groups were assigned from systematic absences as $Pccn$ for **1** and **2**, $P4/ncc$ for **3**. Unit cell and profile refinements were carried out using the Pawley method, and led to good fit ($\chi^2 = 0.050$ for **1**, 0.089 for **2**, and 0.042 for **3**) for these lattice parameters and space groups. Structure solution was carried out by the simulated annealing method with the program DASH (W. I. F. David, K. Shankland, K. J. van de Streek, E. Pidcock, W. D. S. Motherwell, J. C. Cole, *J. Appl. Crystallogr.*, **2006**, *39*, 910-915). Rigid groups: $[\text{Mn}(\text{salen})][\text{Pt}(\text{CN})_4(0.18\text{I}_2)]_{0.5}$ in which I-Pt-CN, CN-Mn-O were allowed to rotate in the asymmetric unit, were introduced by using a constrained Z-matrix description for **1–3**. During annealing, 25 runs of 1×10^7 Monte Carlo moves

each were performed. The best structure obtained (Profile $\chi^2 = 2.27$ for **1**, 0.64 for **2**, and 0.40 for **3**) was taken as the starting structural model for Rietveld refinement.

The Rietveld refinements of **1-3** were performed with the program RIETAN-FP (F. Izumi, K. Momma, *Solid State Phenom.*, **2007**, *130*, 15-20) and VESTA (K. Momma, F. Izumi, *J. Appl. Crystallogr.*, **2008**, *41*, 653-658). Restraints but no constraints for all bond lengths were employed to maintain the molecular geometry. Atomic displacement parameters were refined isotropically with uniform values for **1** and **2**, and with uniform values on C and N with different values on Pt, I, and Mn for **3**. Occupancies of iodine were fixed with determined values from the elemental analysis and TGA data.

Final Rietveld refinement result for **1**: Orthorhombic *Pccn*, $a = 14.682(1) \text{ \AA}$, $b = 14.687(1) \text{ \AA}$, $c = 17.0960(8) \text{ \AA}$, $V = 3686.6(5) \text{ \AA}^3$, $R_{wp} = 1.351\%$ ($R_e = 5.833\%$), $R_p = 1.001\%$, $R_B = 8.016\%$, $R_F = 4.271\%$; 5651 profile points (2θ range, 3.50 to 60.0°); 119 refined variables. The result is shown in Figure S1(a). CCDC deposit number: 1863727.

Final Rietveld refinement result for **2**: Orthorhombic *Pccn*, $a = 14.7030(4) \text{ \AA}$, $b = 14.4342(5) \text{ \AA}$, $c = 17.5493(9) \text{ \AA}$, $V = 3724.4(2) \text{ \AA}^3$, $R_{wp} = 2.815\%$ ($R_e = 7.779\%$), $R_p = 1.824\%$, $R_B = 5.729\%$, $R_F = 2.244\%$; 5651 profile points (2θ range, 3.50 to 60.0°); 92 refined variables. The result is shown in Figure S1(b). CCDC deposit number: 1863728.

Final Rietveld refinement result for **3**: Tetragonal *P4/ccn*, $a = b = 14.5515(1) \text{ \AA}$, $c = 17.6600(2) \text{ \AA}$, $V = 3739.44(7) \text{ \AA}^3$, $R_{wp} = 1.952\%$ ($R_e = 9.389\%$), $R_p = 1.426\%$, $R_B = 4.942\%$, $R_F = 2.369\%$; 5651 profile points (2θ range, 3.50 to 60.0°); 85 refined variables. The result is shown in Figure S1(c). CCDC deposit number: 1863726.

DFT calculation

All geometry optimizations were carried out by density functional theory (DFT) with M06 functional (Y. Zhao and D. G. Truhlar, *Theor. Chem. Account* 2008, **120**, 215-241) using Gaussian 09 E.01 (Gaussian 09, Revision **E.01**, M. J. Frisch, G. W. Trucks, H. B. Schlegel, G. E. Scuseria, M. A. Robb, J. R. Cheeseman, G. Scalmani, V. Barone, B. Mennucci, G. A. Petersson, H. Nakatsuji, M. Caricato, X. Li, H. P. Hratchian, A. F. Izmaylov, J. Bloino, G. Zheng, J. L. Sonnenberg, M. Hada, M. Ehara, K. Toyota, R.

Fukuda, J. Hasegawa, M. Ishida, T. Nakajima, Y. Honda, O. Kitao, H. Nakai, T. Vreven, J. A. Montgomery, Jr., J. E. Peralta, F. Ogliaro, M. Bearpark, J. J. Heyd, E. Brothers, K. N. Kudin, V. N. Staroverov, R. Kobayashi, J. Normand, K. Raghavachari, A. Rendell, J. C. Burant, S. S. Iyengar, J. Tomasi, M. Cossi, N. Rega, J. M. Millam, M. Klene, J. E. Knox, J. B. Cross, V. Bakken, C. Adamo, J. Jaramillo, R. Gomperts, R. E. Stratmann, O. Yazyev, A. J. Austin, R. Cammi, C. Pomelli, J. W. Ochterski, R. L. Martin, K. Morokuma, V. G. Zakrzewski, G. A. Voth, P. Salvador, J. J. Dannenberg, S. Dapprich, A. D. Daniels, Ö. Farkas, J. B. Foresman, J. V. Ortiz, J. Cioslowski and D. J. Fox, Gaussian, Inc., Wallingford CT, 2009). We employed the models as shown in Fig. S5. The distances between Pt and Pt were kept at experimental values of **1** and **3**, namely 8.373 Å for model 1 and 8.768 Å for model 2 during optimization. Basis set of SDD with replacing core electrons with the effective core potential of the Stuttgart-Dresden-Bonn (J. H. Bak, V. D. Le, J. Kang, S. H. Wei and Y. H. Kim, *J. Phys. Chem. C* 2012, **116**, 7386.) was employed for Pt and I, and aug-cc-pVTZ basis set is used for other atoms. To investigate the origin of the absorption observed in **3**, time-dependent DFT (TD-DFT) was also used together with the same basis set as the case of optimization.

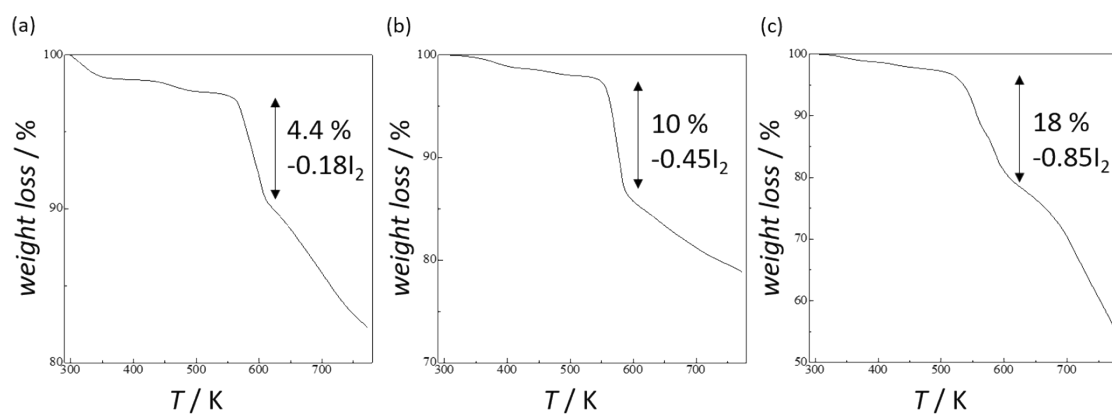


Figure S1 TGA results for (a) **1**, (b) **2** and (c) **3**.

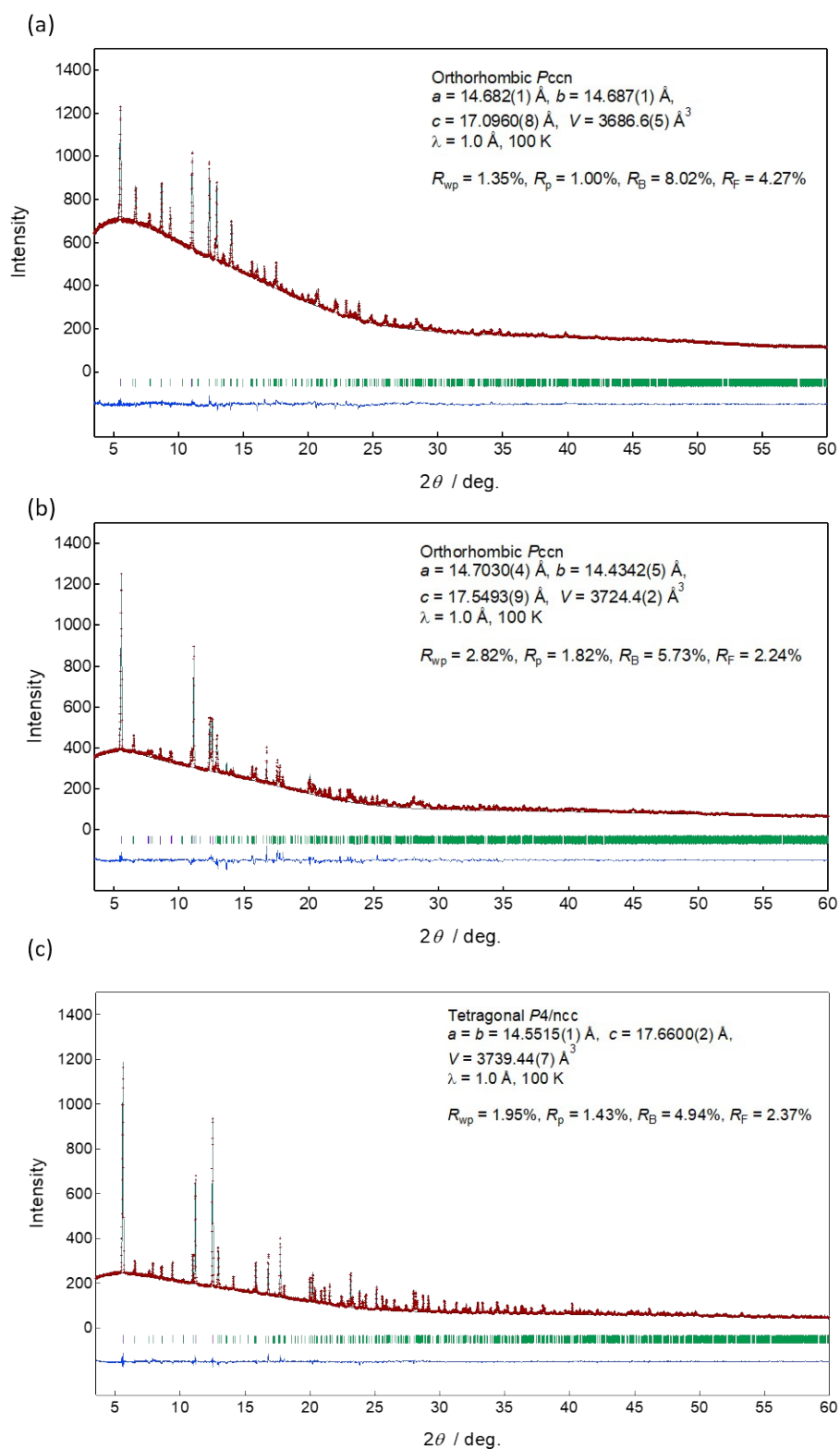


Figure S2 Experimental (red), calculated (black), and difference (blue) PXRD profiles and Bragg positions (green) from the final Rietveld refinements of (a) **1**, (b) **2**, and (c) **3**.

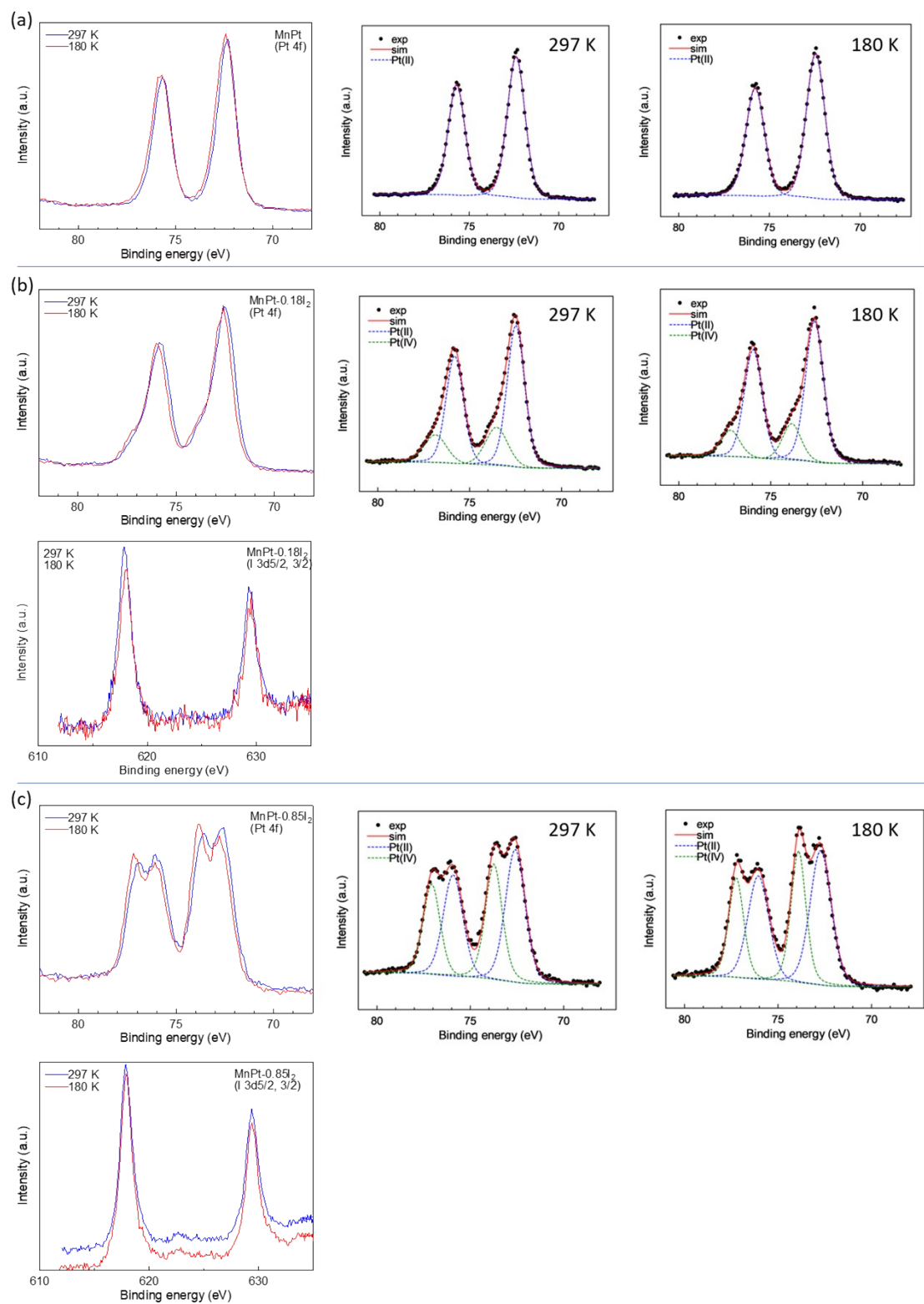


Figure S3 XPS results for Pt (4f) and I (3d) at 297 K (blue line) and 180 K (red line); (a) $[\text{Mn}(\text{salen})]_2[\text{Pt}(\text{CN})_4]$, (b) **1** and (c) **3**.

Table S1. XPS results.

	<i>T</i> / K	Component	Binding Energy (Pt 4f _{7/2}) (eV)	Binding Energy (Pt 4f _{5/2}) (eV)	Area ratio (%)
[Mn(salen)] ₂ [Pt(CN) ₄]	297	Pt ^{II}	72.38	75.71	100
		Pt ^{IV}			
	180	Pt ^{II}	72.45	75.78	100
		Pt ^{IV}			
1	297	Pt ^{II}	72.42	75.75	73.8
		Pt ^{IV}	73.48	76.81	26.1
	180	Pt ^{II}	72.62	75.95	78.2
		Pt ^{IV}	73.86	77.19	21.8
3	297	Pt ^{II}	72.59	75.92	56.2
		Pt ^{IV}	73.74	77.11	43.8
	180	Pt ^{II}	72.72	76.05	57.6
		Pt ^{IV}	73.91	77.24	42.4

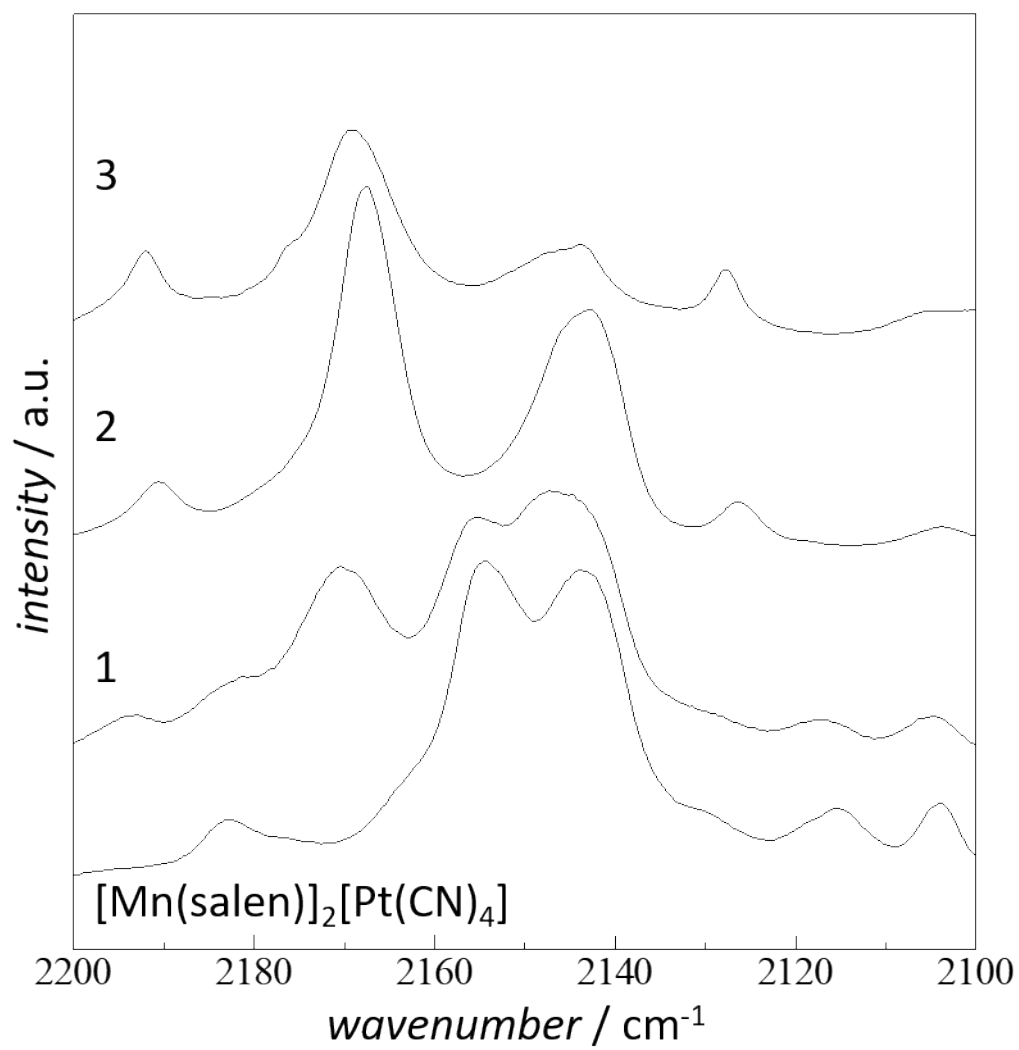


Figure S4 IR spectra for **1–3** and $[\text{Mn}(\text{salen})_2][\text{Pt}(\text{CN})_4]$.

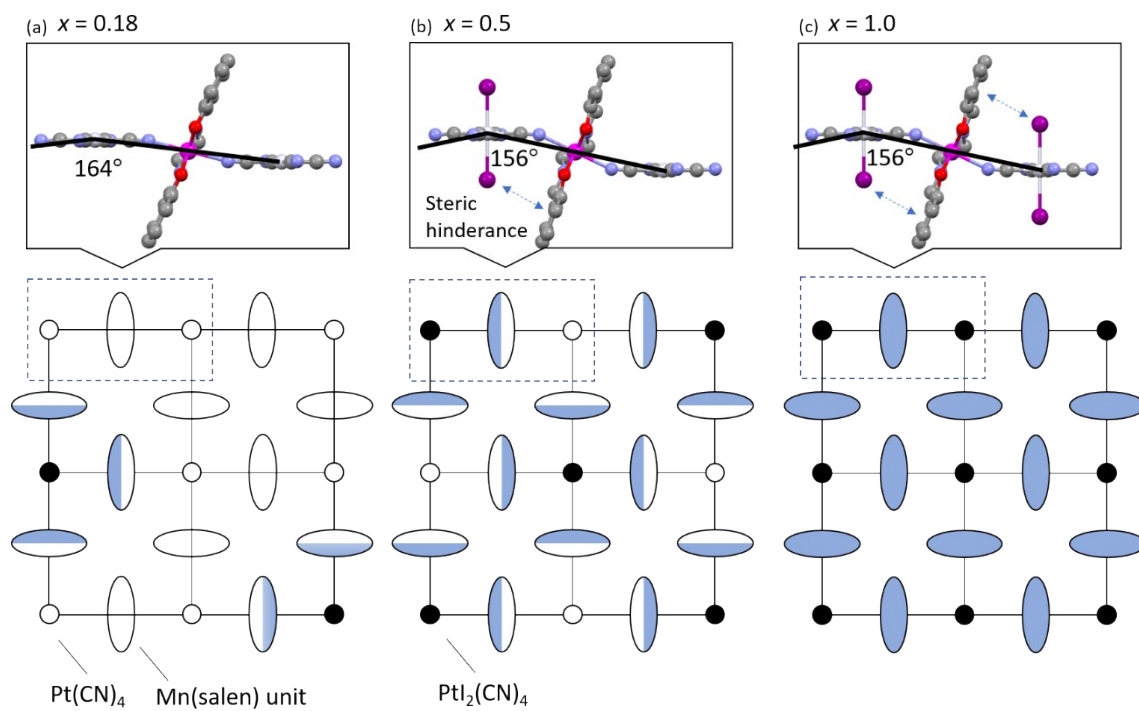


Figure S5 Schematic images for structural transformations with increasing iodine contents in $[\text{Mn}(\text{salen})]_2[\text{Pt}^{\text{II}}(\text{CN})_4]_{1-x}[\text{Pt}^{\text{IV}}(\text{CN})_4(\text{I}_2)]_x$. (a) $x = 0.18$, (b) $x = 0.5$ and (c) $x = 1.0$.

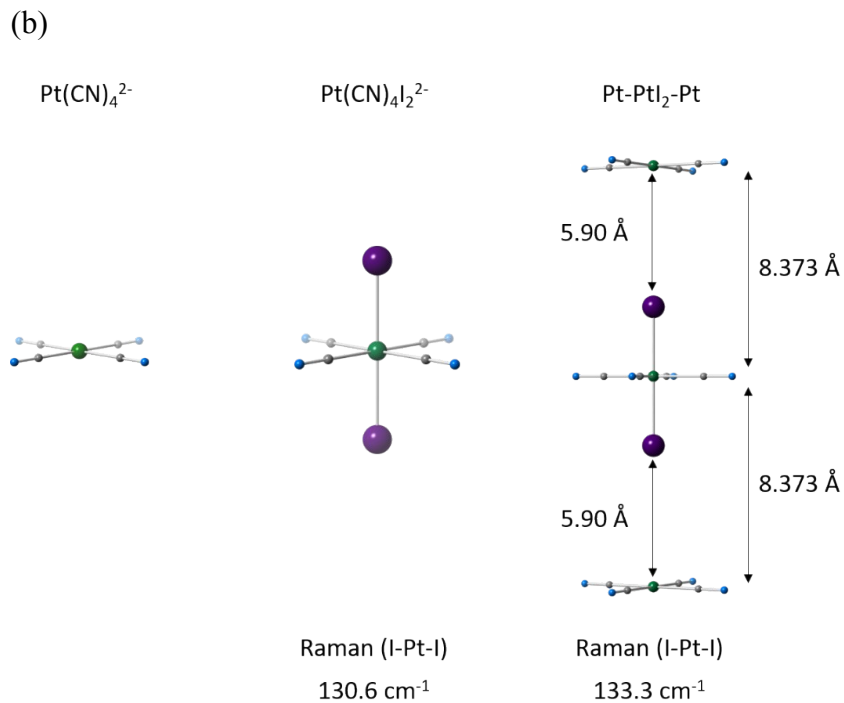
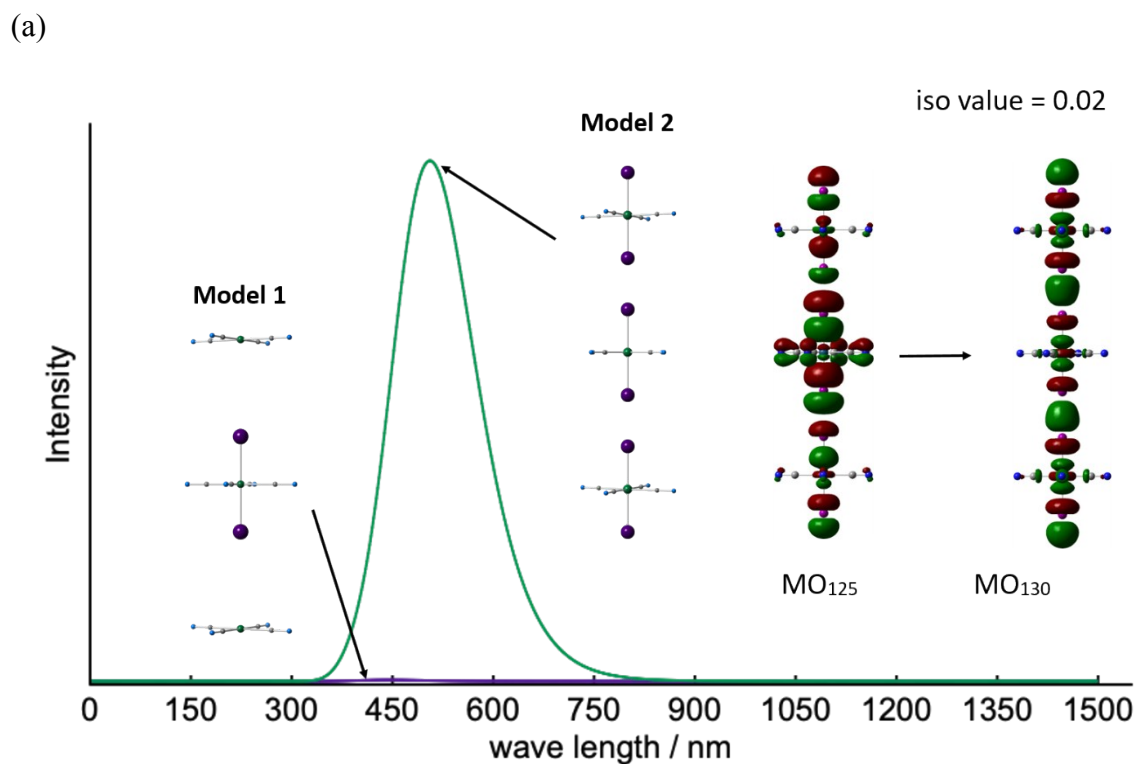


Figure S6 (a) Model units for the DFT calculations and simulated absorption bands. (b) Simulated Raman bands for the I-Pt-I units.

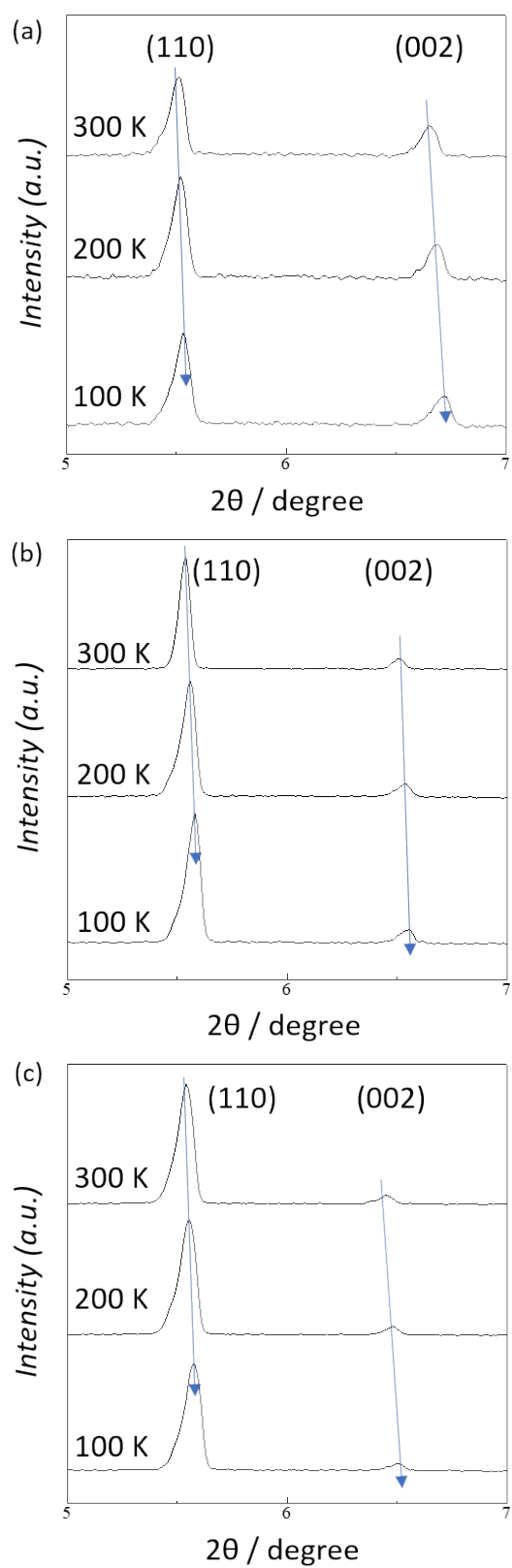


Figure S7 VT-XRPD for (a) **1**, (b) **2** and (c) **3**.

Table S2. Unit cells of **1–3** at various temperatures, indexed by Pawley refinements**Compound 1**

Temp. / K	Space group		$a / \text{Å}$	$b / \text{Å}$	$c / \text{Å}$	$V / \text{Å}^3$	fit χ^2
100	Orthorhombic	<i>Pncc</i>	14.667	14.664	17.085	3674.59	0.050
200	Tetragonal	<i>P4/ncc</i>	14.693	(= a)	17.161	3704.61	0.011
300	Tetragonal	<i>P4/ncc</i>	14.718	(= a)	17.232	3732.67	0.018

Compound 2

Temp. / K	Space group		$a / \text{Å}$	$b / \text{Å}$	$c / \text{Å}$	$V / \text{Å}^3$	fit χ^2
100	Orthorhombic	<i>Pncc</i>	14.699	14.441	17.547	3724.77	0.089
200	Tetragonal	<i>P4/ncc</i>	14.629	(= a)	17.600	3766.55	0.070
300	Tetragonal	<i>P4/ncc</i>	14.679	(= a)	17.662	3805.57	0.070

Compound 3

Temp. / K	Space group		$a = b / \text{Å}$	$c / \text{Å}$	$V / \text{Å}^3$	fit χ^2
100	Tetragonal	<i>P4/ncc</i>	14.552	17.660	3739.60	0.042
200	Tetragonal	<i>P4/ncc</i>	14.594	17.697	3769.03	0.030
300	Tetragonal	<i>P4/ncc</i>	14.642	17.868	3813.53	0.014

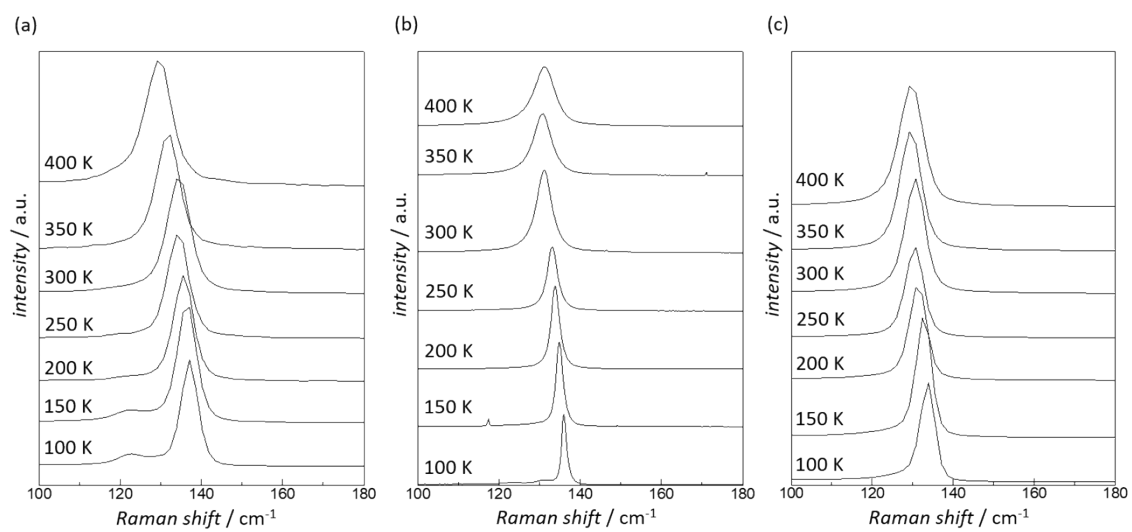


Figure S8 VT-Raman spectra for (a) **1**, (b) **2** and (c) **3**.